

Recurrent Fusion of the Genes for High-mobility Group AT-hook 2 (*HMGA2*) and Nuclear Receptor Co-repressor 2 (*NCOR2*) in Osteoclastic Giant Cell-rich Tumors of Bone

IOANNIS PANAGOPOULOS¹, KRISTIN ANDERSEN¹, LUDMILA GORUNOVA¹,
MARIUS LUND-IVERSEN², INGVILD LOBMAIER² and SVERRE HEIM^{1,3}

¹Section for Cancer Cytogenetics, Institute for Cancer Genetics and Informatics,
The Norwegian Radium Hospital, Oslo University Hospital, Oslo, Norway;

²Department of Pathology, The Norwegian Radium Hospital, Oslo University Hospital, Oslo, Norway;

³Institute of Clinical Medicine, Faculty of Medicine, University of Oslo, Oslo, Norway

Abstract. *Background/Aim:* Chimeras involving the high-mobility group AT-hook 2 gene (*HMGA2* in 12q14.3) have been found in lipomas and other benign mesenchymal tumors. We report here a fusion of *HMGA2* with the nuclear receptor co-repressor 2 gene (*NCOR2* in 12q24.31) repeatedly found in tumors of bone and the first cytogenetic investigation of this fusion. *Materials and Methods:* Six osteoclastic giant cell-rich tumors were investigated using G-banding, RNA sequencing, reverse transcription polymerase chain reaction, Sanger sequencing, and fluorescence in situ hybridization. *Results:* Four tumors had structural chromosomal aberrations of 12q. The pathogenic variant c.103_104GG>AT (p.Gly35Met) in the H3.3 histone A gene was found in a tumor without 12q aberration. In-frame *HMGA2–NCOR2* fusion transcripts were found in all tumors. In two cases, the presence of an *HMGA2–NCOR2* fusion gene was confirmed by FISH on metaphase spreads. *Conclusion:* Our results demonstrate that a subset of osteoclastic giant cell-rich tumors of bone are characterized by an *HMGA2–NCOR2* fusion gene.

This article is freely accessible online.

Correspondence to: Ioannis Panagopoulos, Section for Cancer Cytogenetics, Institute for Cancer Genetics and Informatics, The Norwegian Radium Hospital, Oslo University Hospital, Montebello, PO Box 4954 Nydalen, NO-0424 Oslo, Norway. Tel: +47 22782362, email: ioannis.panagopoulos@rr-research.no

Key Words: Benign bone tumor, non-ossifying fibroma, giant cell tumor of bone, osteoclastic giant cell-rich tumors of bone, cytogenetics, chromosomal aberrations, *HMGA2*, *NCOR2*, *HMGA2–NCOR2* fusion gene.

According to the latest edition of the World Health Organization classification of soft tissue and bone tumors, published in 2020, aneurysmal bone cyst, non-ossifying fibroma, and giant cell tumor of bone comprise a group of osteoclastic giant cell-rich tumors (1, 2). Their common feature is that they contain reactive osteoclast-type multinucleated giant cells (1, 2).

Aneurysmal bone cysts are pathogenetically characterized by rearrangements of chromosome band 17p13 targeting the ubiquitin-specific protease 6 gene (*USP6* or *Tre2*) resulting in fusions in which *USP6* is the 3' moiety, but where the promoter of *USP6* is replaced by a stronger promoter from the partner fusion gene so that *USP6* becomes transcriptionally up-regulated (3-8). The chromosome translocation t(16;17)(q22;p13) is the most frequent cytogenetic aberration reported (21%) in aneurysmal bone cysts with an abnormal karyotype (9). It generates a fusion gene in which the strong promoter of the cadherin 11 gene (*CDH11*) from 16q21 fuses with the *USP6* coding sequence from 17p13 (6, 7) leading to a *CDH11–USP6* chimera in which the *USP6* gene is transcriptionally up-regulated (3, 4).

In non-ossifying fibromas, activating mutations in the mitogen-activated protein kinase pathway were recently found in 81% of examined tumors (10, 11). Using DNA sequencing methodology, mutually exclusive pathogenic mutations were identified in the *KRAS* proto-oncogene (in 12p12), fibroblast growth factor receptor 1 gene (*FGFR1* in 8p11), and neurofibromin 1 gene (*NF1* in 17q11) (10, 11). Giant cell tumors of bone are genetically characterized by pathogenic variations in the 35th codon (exon 2) of the H3.3 histone A gene (*H3-3A* alias *H3F3A*) (12-20). The pathogenic variation c.103G>T, p.Gly35Trp (NM_002107.4, NP_002098.1, COSM1732355) is found in most giant cell tumors, where it is detected only in cells with a fibroblast-

Table I. Clinicopathological data on the tumors with high-mobility group AT-hook 2 and nuclear receptor co-repressor 2 genes (*HMGA2-NCOR2*) fusion.

Case	Gender/age, years	Diagnosis	Pathogenic variation in exon 2 of <i>H3-3A</i>	Tumor location	Fusion transcript	Karyotype
1	F/37	Benign fibrous histiocytoma	None	TH9 vertebra	<i>HMGA2</i> ex3– <i>NCOR2</i> ex16	46,XX,?add(12)(q24),del(20)(q11)[11]/47~49,XX,+7,+18[cp5]/46,XX[4]
2	F/40	Benign fibrous histiocytoma	None	Os pubis	<i>HMGA2</i> ex4– <i>NCOR2</i> ex16	46,XX,der(6)(6pter->6q21::12q13->12q?:?:12q24->12q14:),add(12)(q13)[7]/46,XX[10]
3	M/36	Giant cell tumor of bone with components of secondary aneurysmal bone cyst	None	Distal tibia	<i>HMGA2</i> ex4– <i>NCOR2</i> ex16	46,XY,t(12;12)(q13~15;q24)[9]/46,XY[3]
4	F/16	Giant-cell tumor of bone after treatment with denosumab	None	Scapula	<i>HMGA2</i> ex4– <i>NCOR2</i> ex16	46,XX,der(2)(2pter->2q37::12q24->12q14:),del(12)(q14~15)[5]/47,idem,+17[3]/46,idem,add(17)(q25)[3]/46,XX[2]
5a	M/20	Giant cell tumor of bone with components of secondary aneurysmal bone cyst	c.103_104GG>AT (p.Gly35Met)	Distal left femur	<i>HMGA2</i> ex4– <i>NCOR2</i> ex16	a: 45,XY,-4[6]/46,idem,+r[cp13]/46,XY[2] b: 46,XY,-4,+r[5]/46,XY[7] c: 46~47,XY,-4,+r[cp9]/46,XY[2]
6a	M/21	Giant cell tumor of bone	None	L5 vertebra	<i>HMGA2</i> ex3– <i>NCOR2</i> ex16	a: 46,XY b: 46,XY

F: Female; M: male. All samples were negative for immunohistochemistry against H3.3 G35W.

like appearance, not in giant cells or their precursors (12-18). Other mutations found in the same codon of *H3-3A* are p.Gly35Leu, p.Gly35Val, p.Gly35Met, p.Gly35Glu, and p.Gly35Arg (12-18). Giant cell tumors of bone without mutation in *H3-3A* have also been reported (13, 14).

In the present study, we describe six osteoclastic giant cell-rich tumors that carried a fusion between the genes coding for high-mobility group AT-hook 2 (*HMGA2*) and nuclear receptor co-repressor 2 (*NCOR2*).

Materials and Methods

Ethics statement. The study was approved by the Regional Ethics Committee (Regional komité for medisinsk forskningsetikk Sør-Øst, Norge, <http://helseforskning.etikkom.no>). All clinical information has been de-identified.

Tumor description. Table I shows the patients' gender, age, diagnosis, and tumor location. The patients were three males and three females. The age range was from 16 to 40 years with a median of 28.5 years. The tumors in patients 1 and 2 were diagnosed as benign fibrous histiocytoma of bone. In patients 3 to 6, the tumors were diagnosed as giant cell tumor of bone. Immunohistochemistry showed that all tumors were negative for H3.3 G35W (previously written as G34W).

Patient 1 was a 37-year-old woman with back pain for 2 years and neurological symptoms. A tumor in the TH9 vertebra was found with computed tomography. Core-needle biopsy showed a fibrous lesion in the bone, with macrophages and scattered giant cells. The diagnosis was benign fibrous histiocytoma of bone (Figure 1A). The lesion was H3.3 G35W IHC-negative (Figure 1B). Examination of the curetted specimen confirmed the diagnosis.

Patient 2 was a 40-year-old woman. The tumor was located in the pubic bone. It was H3.3 G35W IHC-negative and diagnosed as a benign fibrous histiocytoma of bone.

The tumors of patients 3 and 5 were located in the distal tibia and distal femur, respectively. They were diagnosed as giant cell tumors of bone with components of aneurysmal bone cyst.

Patient 4 was a 16-year-old girl. She had had shoulder pain for 9 months. An expansive lesion in the scapula with bone destruction was found. Examination of a core-needle biopsy showed tumor tissue with scattered giant cells against a background of bland-looking mononuclear cells, scattered macrophages, and hemosiderin deposits (Figure 1C). Despite negative IHC analysis for H3.3 G35W (Figure 1D), a diagnosis of giant cell tumor of bone was reached and the patient received denosumab for 4 months followed by curettage. The histological picture of fibrous tumor tissue with mononuclear cells and scattered giant cells (Figure 1C) was consistent with the diagnosis of a giant cell tumor.

In patient 6, a tumor was found in the L5 vertebra. Although it was H3.3 G35W IHC-negative, a diagnosis of giant cell tumor of bone was reached.

G-Banding and karyotyping. The methods used to investigate the tumors cytogenetically were described elsewhere (21). Briefly, a part of resected tumor was minced with scalpels into 1-2 mm fragments and then enzymatically disaggregated with collagenase II (Worthington, Freehold, NJ, USA). The resulting cells were cultured, harvested, and processed for cytogenetic examination using standard techniques (22). A G-banding pattern of chromosomes was obtained using Wright's stain (Sigma-Aldrich, St Louis, MO, USA) (22). Metaphases were analyzed and karyograms prepared using the CytoVision computer-assisted karyotyping system (Leica Biosystems, Newcastle upon Tyne, UK). The karyotypes were described according to the International System for Human Cytogenomic Nomenclature (23).

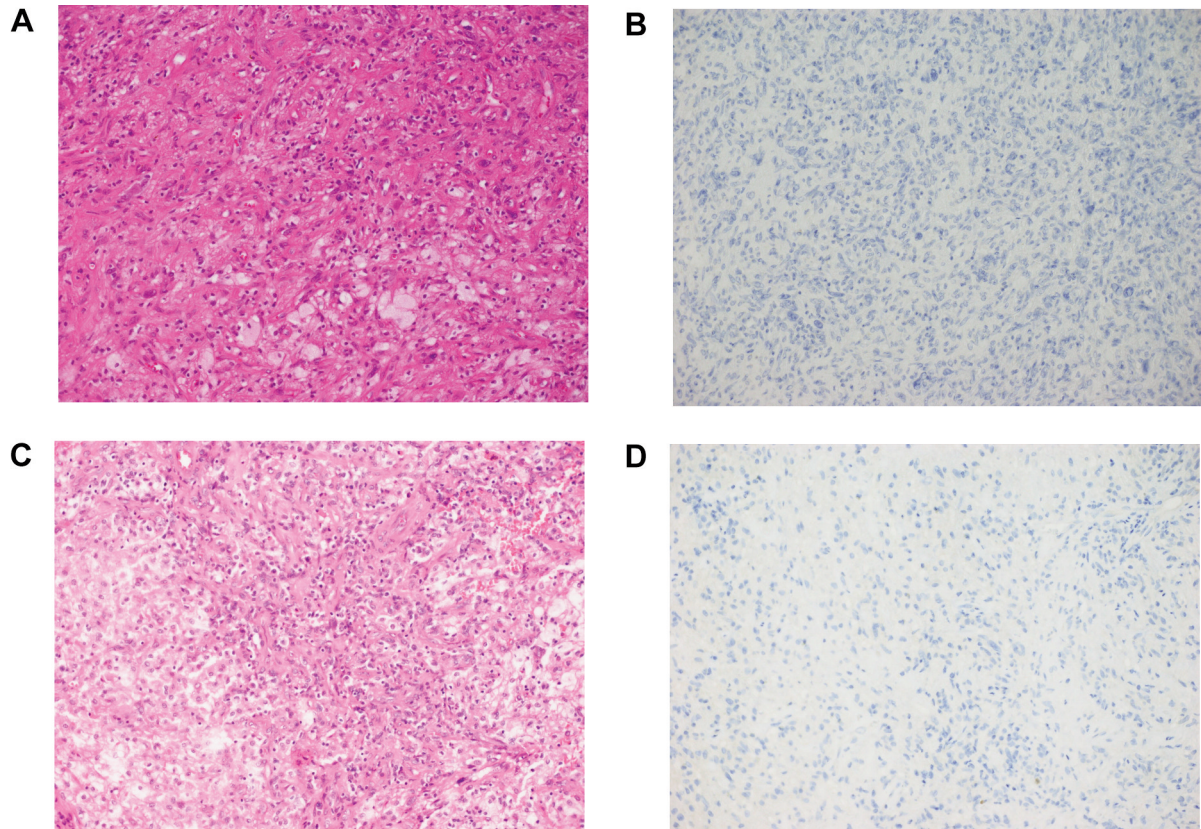


Figure 1. Microscopic examination of osteoclastic giant cell-rich tumor of bone from case 1 (A and B) and case 4 (C and D). A: The tumor tissue consisted of mononuclear cells with eosinophilic cytoplasm and small, round to oval nuclei. Throughout the tumor tissue there were scattered areas of foamy macrophages and a few multinuclear giant cells (the latter not visible in the image), hematoxylin and eosin (H&E), $\times 20$ objective. B: Immunohistochemical examination against H3.3 G35W (previously written as G34W) showing cell nuclei within the tumor tissue that were negative for H3.3 G35W. C: The histological picture was dominated by mononuclear cells without atypia. The nuclei were round to oval, and the cytoplasm had indistinct borders. Throughout the lesion there were areas with foamy macrophages. Very few giant cells were seen, H&E, $\times 20$ objective. D: Immunohistochemical examination showed that nuclei in the tumor tissue were negative for H3.3 G35W.

Sanger sequencing for detection of pathogenic variation in exon 2 of the *H3-3A* gene. Genomic DNA from tumor samples was extracted using a Maxwell RSC Instrument and a Maxwell RSC Tissue DNA Kit (Promega, Madison, WI, USA) and subsequently quantified with Quantus Fluorometer and the QuantiFluor ONE dsDNA System (Promega). Extracted DNA (100-150 ng) was used as polymerase chain reaction (PCR) template for detection of possible pathogenic variation in exon 2 of the *H3-3A* gene (NCBI reference sequence: NM_002107.4). The primers M13For-H3F3A-Ex2-F2 and M13Rev-H3F3A-Ex2-R2 (Table II), together with the BigDye Direct Cycle Sequencing Kit, were used to perform both PCR and cycle (Sanger) sequencing according to the company's recommendations (ThermoFisher Scientific, Waltham, MA, USA). The sequences obtained by Sanger sequencing were compared with the NCBI reference sequence NM_002107.4.

RNA sequencing. Total RNA was extracted from frozen tumor tissue adjacent to that used for cytogenetic analysis and histological examination using miRNeasy Mini Kit (Qiagen, Hilden, Germany).

RNA sequencing was performed on cases 1 and 2 (Table I). For this purpose, 1 μg of total RNA was sent to the Genomics Core Facility at the Norwegian Radium Hospital, Oslo University Hospital for high-throughput paired-end RNA sequencing. A total of 89×10^6 and 107×10^6 76-bp-length reads were obtained from the tumors of cases 1 and 2, respectively. FASTQC software was used for quality control of the raw sequence data (available online at: <http://www.bioinformatics.babraham.ac.uk/projects/fastqc/>). Fusion transcripts were found using FusionCatcher software (24, 25). The "grep" command was also used to search the fastq files of the sequence data for the *HMGA2-NCOR2* fusion sequence. The principle of this approach has been described in detail elsewhere (26-28). The search terms were "AGGAAATGGCAGCAGCAA" and "AGGAAATGGCAGCAACAA" for case 1 and "CCTGCTCAGCAGCAGCAA" and "CCTGCTCAGCAGCAACAA" for case 2.

Reverse transcription (RT)PCR and Sanger sequencing analyses. The primers used for PCR amplification and Sanger sequencing analyses are shown in Table II. The methodologies for cDNA

Table II. Primers used for polymerase chain reaction amplification and Sanger sequencing analyses. M13 forward primer (*TGTAACGACGGCCAGT*) and M13 reverse primer (*CAGGAAACAGCTATGACC*) sequences are shown in italics.

Gene name (gene symbol)	Name: Sequence (5'→3')	Reference sequence: Position	Chr. band
H3.3 histone A (<i>H3-3A</i>)	M13For-H3F3A-Ex2-F2: <i>TGTAACGACGGCCAGT</i> - CAGGAAAAGTTGTATGTTTGGTAGTTGC	NC_000001.11: 226,064, 268-226,064,295	1q42.12
H3.3 histone A (<i>H3-3A</i>)	M13Rev-H3F3A-Ex2-R2: <i>CAGGAAACAGCTATGACC</i> - AAAGCAAAAAGTTTCCTGTTATCCATC	NC_000001.11: 226,064, 547-226,064,574	1q42.12
High mobility group AT-hook 2 (<i>HMGA2</i>)	<i>HMGA2</i> -846F1: CCACTTCAGCCC AGGGACAACCT	NM_003483.4: 846-868	12q14.3
High mobility group AT-hook 2 (<i>HMGA2</i>)	<i>HMGA2</i> -925F1: ACCAACCGGTGA GCCCTCTCCTA	NM_003483.4: 925-947	12q14.3
Nuclear receptor co-repressor 2 (<i>NCOR2</i>)	<i>NCOR2</i> -2076R1: CTCCTTGTCGT TCTCCACCTCCG	NM_006312.6: 2099-2076	12q24.31
Nuclear receptor co-repressor 2 (<i>NCOR2</i>)	<i>NCOR2</i> -2127R1: TCGTCGTTG TCCTCCCCTGAGG	NM_006312.6: 2148-2127	12q24.31

Chr: Chromosomal.

Table III. BAC probes used for fluorescence in situ hybridization experiments in order to detect the high-mobility group AT-hook 2 and nuclear receptor co-repressor 2 (*HMGA2-NCOR2*) fusion gene. The positions of the *HMGA2* and *NCOR2* genes are also given.

BAC clone	Accession number	Chr mapping	Targeted gene	Position on GRCh38/hg38 assembly	Labelling
RP11-185K16	AQ418927.1 and AQ418930.1	12q14.3	<i>HMGA2</i>	Chr12:65427017-65594623	Fluorescein-12-dCTP (Green)
RP11-30I11	B87811.1 and B87812.1	12q14.3	<i>HMGA2</i>	Chr12:65498459-65669659	Fluorescein-12-dCTP (Green)
RP11-662 G15	AQ411650 and AQ411760	12q14.3	<i>HMGA2</i>	Chr12:65608717-65818177	Fluorescein-12-dCTP (Green)
	NM_003483.6	12q14.3	<i>HMGA2</i>	Chr12:65824483-65966291	
RP11-118B13	AQ347872.1, AQ347869.1, and AC135255.2	12q14.3	<i>HMGA2</i>	Chr12:65964922-66109206	Fluorescein-12-dCTP (Green)
RP11-745O10	AC078927.20	12q14.3	<i>HMGA2</i>	Chr12:66083023-66208799	Fluorescein-12-dCTP (Green)
RP11-263A04	AC025603.1	12q14.3	<i>HMGA2</i>	Chr12:66246378-66412442	Fluorescein-12-dCTP (Green)
RP11-522N14	AC026358.36	12q24.31	<i>NCOR2</i>	Chr12:124142622-124286745	Texas Red-5-dCTP (Red)
RP11-408I18	AC073916.41	12q24.31	<i>NCOR2</i>	Chr12:124286746-124490024	Texas Red-5-dCTP (Red)
	NM_006312.6	12q24.31	<i>NCOR2</i>	Chr12:124324415-124495252	
RP11-83B20	AC073592.11	12q24.31	<i>NCOR2</i>	Chr12:124499239-124658361	Texas Red-5-dCTP (Red)

Chr: Chromosome.

synthesis, RT-PCR amplification, and Sanger sequencing were described elsewhere (29, 30). For the first outer PCR amplification, the primer combination *HMGA2*-846F1/*NCOR2*-2127R1 was used. For the second inner PCR, the primer combination *HMGA2*-925F1/*NCOR2*-2076R1 was used. The Basic Local Alignment Search Tool (BLAST) was used to compare the sequences obtained by Sanger sequencing with the NCBI reference sequences NM_003483.4 (*HMGA2*) and NM_006312.6 (*NCOR2*) (31).

Fluorescence in situ hybridization (FISH). For the detection of *HMGA2-NCOR2* fusion gene, a homemade double-fusion FISH probe was used. The BAC probes were purchased from the BACPAC Resource Center operated by BACPAC Genomics, Emeryville, CA, USA (<https://bacpacresources.org/>) (Table III). The probes for *HMGA2* were labelled with fluorescein-12-dCTP (PerkinElmer, Boston, MA, USA) to obtain a green signal. The probes for *NCOR2* were labelled with Texas Red-5-dCTP (PerkinElmer) to obtain a red

signal. Detailed information on the FISH procedure was given elsewhere (30, 32). Fluorescent signals were captured and analyzed using the CytoVision system (Leica Biosystems).

Results

Karyotyping. Cytogenetic examination revealed chromosomal aberrations in five tumors whereas a normal male karyotype was obtained in both samples from case 6 (Table I). The tumors had pseudo- or near-diploid karyotypes. The dominating feature was an aberration of the q arm of chromosome 12 found in four cases (Table I, Figure 2). In case 1, G-banding analysis detected two cytogenetically unrelated clones: One had the chromosome abnormalities add(12)(q24) and del(20)(q11) whereas the second, composite clone had one

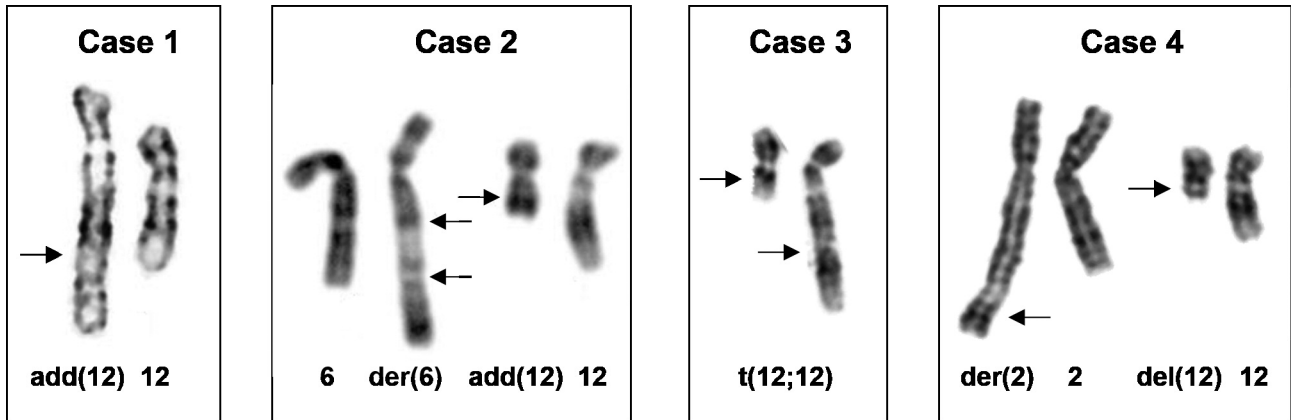


Figure 2. G-Banding analyses of osteoclastic giant cell-rich tumors of bone. Partial karyotypes of tumors (cases 1-4) with 12q anomalies are presented. From case 1, the abnormal chromosome *add(12)(q24)* together with the normal chromosome 12 are shown. From case 2, the two abnormal chromosomes, *der(6)(6pter->6q21::12q13->12q?::12q24->12q14:)* and *add(12)(q13)*, are shown together with normal chromosomes 6 and 12. From case 3, the two derivative chromosome 12 from the translocation *t(12;12)(q13~15;q24)* are shown. From case 4, the two abnormal chromosomes, *der(2)(2pter->2q37::12q24->12q14:)* and *del(12)(q14~15)*, are shown together with the normal chromosomes 2 and 12. Arrows indicate breakpoints.

extra copy of chromosomes 7 and 18. In case 2, a single cytogenetic clone was found with structural aberrations *der(6)(6pter->6q21::12q13->12q?::12q24->12q14:)* and *add(12)(q13)*. In the third case, a balanced translocation *t(12;12)(q13~15;q24)* was found as the only abnormality. In the fourth tumor, three related clones were found connected by the presence of a *der(2)(2pter->2q37::12q24->12q14:)* and a *del(12)(q14~15)*. Finally, the tumor of the fifth case had monosomy 4 and a ring chromosome.

Sanger sequencing of exon 2 of H3-3A. None of the tumors had the pathogenic variation c.103G >T, p.Gly35Trp (NM_002107.4, NP_002098.1, COSM1732355). In the tumor sample from patient 5, the pathogenic variant c.103_104GG>AT (p.Gly35Met) was found (Figure 3).

RNA sequencing. Analysis of the sequencing data with FusionCatcher for case 1 detected an in-frame fusion of exon 3 of *HMGA2* from 12q14 (NCBI reference sequences NM_003483.4) with exon 16 of *NCOR2* from 12q24 (reference sequence NM_006312.6): AGCCACTGGAGAAAAACGG CCAAGAGGCAGACCTAGGAAATGG*CAGCAGCAACA ACAGCAGCAGCAGCAGCAGCAGCAGCAGCAGCAGCAGC. Examining the fastq files of the sequence data using the “grep” command and the search term “AGGAAATGGCAGCA GCAA”, nine sequence reads with the above-mentioned fusion point were found (Table IV), whereas use of the “grep” search with “AGGAAATGGCAGCAACAA” yielded 15 sequence reads with this fusion point. The obtained results agreed with the Sanger sequencing chromatograms, where an AGGAAATGG-CAGCARCAACAR sequence was found at the junction (see below). In case 2, FusionCatcher detected an

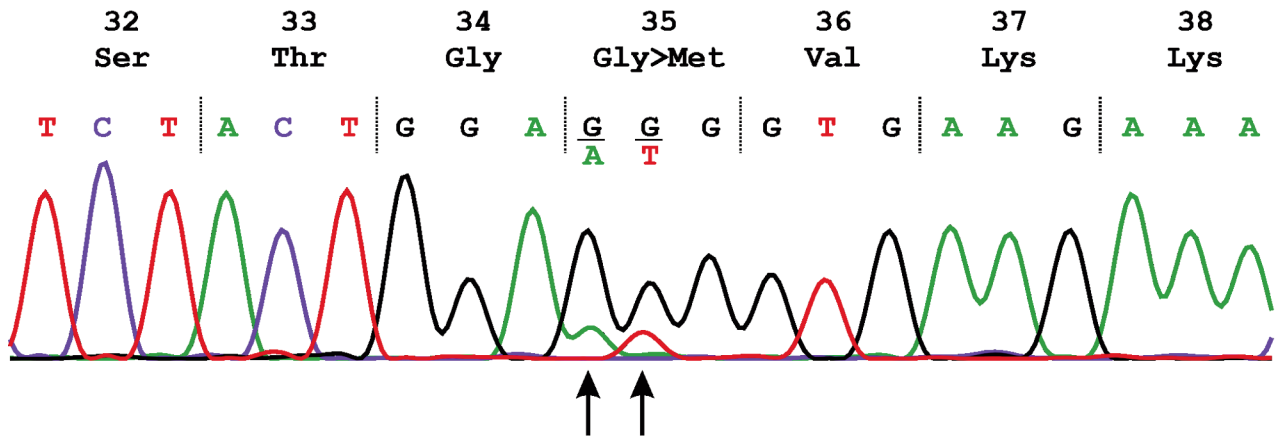
in-frame fusion of exon 4 of *HMGA2* with exon 16 of *NCOR2*: TAGGAAATGGCCACAACAAGTTGTTTCAGAAGAAGCCT GCTCAG*CAGCAGCAACAACAGCAGCAGCAGCAGCA GCAGCAGCAGCAGCAGC. Using the “grep” command and the search term “CCTGCTCAGCAGCAGCAA”, 17 sequence reads with the above-mentioned fusion point were found (Table IV), whereas the “grep” search with term “CCTGCTCAGCAG CAACAA” yielded 16 reads with this fusion point. The results agreed with the Sanger sequencing chromatograms which showed an CCTGCTCAG-CAGCARCAACAR sequence at the junction (see below).

Thus, for cases 1 and 2, FusionCatcher, examination of fastq files of sequence data with the “grep” command, and RT-PCR/Sanger sequencing showed that there was an in-frame insertion/deletion of a CAG triplet in exon 16 of *NCOR2* at the junction of fusion transcripts.

RT-PCR and Sanger sequencing analyses. In cases 1 and 2, RT-PCR with the outer *HMGA2*-846F1/*NCOR2*-2127R1 primer combination amplified a 412-bp and a 445-bp cDNA fragment, respectively (Figure 4A). Nested PCR with the inner primer combination *HMGA2*-925F1/*NCOR2*-2076R1 amplified 284-bp (case 1) and 317-bp (case 2) cDNA fragments (Figure 4B). Sanger sequencing of the amplified fragments showed that they were *HMGA2-NCOR2* chimeric cDNA fragments in which exon 3 of *HMGA2* was fused to exon 16 of *NCOR2* (case 1) or exon 4 of *HMGA2* fused to exon 16 of *NCOR2* (case 2) (Figure 4C), thus confirming the results obtained by RNA sequencing.

In cases 3, 4, and 5, nested PCR amplified a 317-bp cDNA fragment (data not shown). Sanger sequencing of these fragments detected fusion between *HMGA2* exon 4 and

Sanger sequencing with forward primer



Sanger sequencing with reverse primer

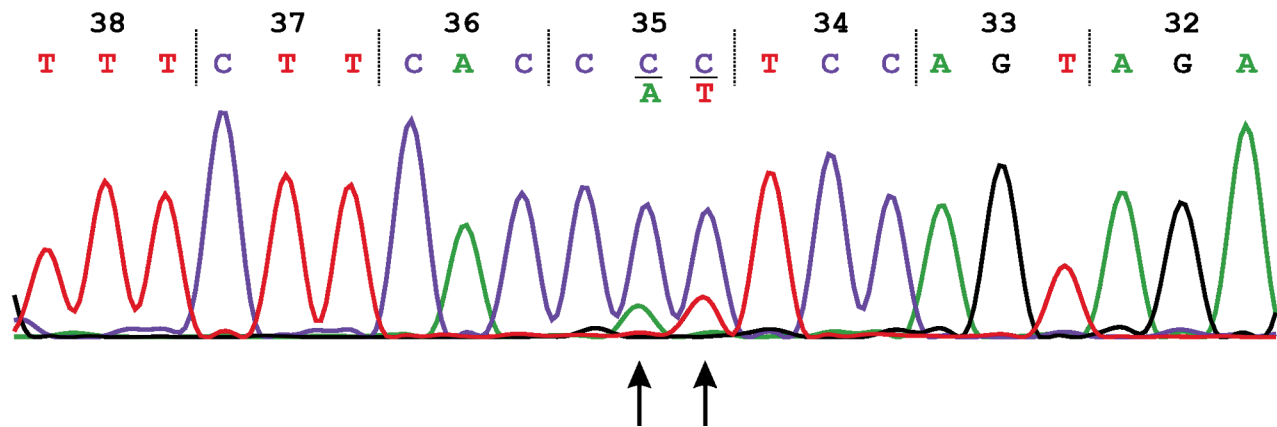


Figure 3. Pathogenic variation in exon 2 of the *H3-3A* gene. Partial sequence chromatograms of DNA amplified fragments from case 5 showing the presence of the pathogenic variant *c.103_104GG>AT* (*p.Gly35Met*) in the tumor.

NCOR2 exon 16 (Table I, Figure 4C). In case 6, nested PCR amplified a 284-bp cDNA fragment in which exon 3 of *HMGA2* was fused to exon 16 of *NCOR2*. At the junction of fusion transcript an in-frame insertion/deletion of a CAG triplet in exon 16 of *NCOR2* was found, similar to cases 1 and 2 (Table I, Figure 4C).

FISH analyses. Metaphase spreads from cases 2, 4, and 5 (sample 5c) were available for FISH analysis with a homemade double *HMGA2-NCOR2* fusion probe consisting of green-labeled *HMGA2* (12q14) and red-labeled *NCOR2* probes (12q24) (Table III, Figure 5A). For case 2, a yellow signal for *HMGA2-NCOR2* fusion as well as a green signal for *HMGA2* were found on the der(6)(6pter->6q21::12q13->12q?::12q24->12q14): (Figure 5B). Green signals for *HMGA2* were seen also on chromosomes 12 and add(12)(q13), suggesting the presence of at least one intact

(normal) *HMGA2* locus in the abnormal metaphases. A red signal for *NCOR2* was found on chromosome 12 (Figure 5B).

In case 4, two fusion signals were found on der(2)(2pter->2q37::12q24->12q14~15) together with a green signal for *HMGA2* and a red signal for *NCOR2* on chromosome 12 (Figure 5B). In case 5, FISH experiments on metaphase spreads with -4 and +r showed normal patterns, in other words, green (*HMGA2*) and red (*NCOR2*) signals on the two chromosomes 12 (Figure 5B).

Discussion

We describe an *HMGA2-NCOR2* fusion transcript found in six osteoclastic giant cell-rich bone tumors in which immunohistochemistry against H3.3 G35W showed that all of them were negative. In one tumor (patient 5), the extremely rare pathogenic variant *c.103_104GG>AT* (*p.Gly35Met*) of the

H3-3A gene was found. This tumor had two cytogenetically unrelated clones: one with monosomy 4 and a ring chromosome with normal patterns for the *HMGA2* and *NCOR2* genes, the other with an *HMGA2-NCOR2* fusion. Thus, we do not know if the p.Gly35Met of the *H3-3A* gene and *HMGA2-NCOR2* fusion occurred in the same clone or not.

In the tumor of cases 1 and 6, the fusion occurred between exons 3 of *HMGA2* and 16 of *NCOR2*, whereas in the other tumors, exon 4 of *HMGA2* was found to be fused to exon 16 of *NCOR2*. Cytogenetically, four tumors had visible rearrangements of 12q, with one of them (case 3) showing a translocation between the two copies of chromosome 12, t(12;12)(q13~15;q24). Since *HMGA2* (in 12q14) is transcribed from centromere to telomere whereas *NCOR2* (in 12q24) is transcribed from telomere to centromere (Figure 4A), neither a simple balanced 12q14;12q24-translocation nor an interstitial deletion del(12)(q14q24) is sufficient to generate the *HMGA2-NCOR2* fusion gene. We therefore believe that the seemingly solitary t(12;12)(q13~15;q24) of case 3 must be accompanied by additional submicroscopic rearrangement(s), probably an inversion, to enable the generation of a functionally competent *HMGA2-NCOR2* fusion on one of the derivative chromosomes 12. A t(12;12)(q14;q24) was reported in a uterine leiomyoma with a complex karyotype (33).

A paracentric inversion, inv(12)(q14q24), with break in intron 3 or 4 of *HMGA2* and a break upstream of exon 16 of *NCOR2*, would move part of the 3'-end partner gene *NCOR2* from 12q24 to 12q14 into the *HMGA2* locus where the fusion then takes place. The FISH results from cases 2 and 4 indicate that such an inversion is accompanied by other chromosomal aberrations, including translocations. In case 2, which had a der(6)(6pter->6q21::12q13->12q?::12q24->12q14:), the fusion signal (yellow) was proximal whereas a green *HMGA2* signal was distal on the der(6). Finally in case 4, a paracentric inversion between 12q14 and 12q24 chromosomal bands, with breakpoints in the *HMGA2* and *NCOR2* loci and translocation of this part of chromosome 12 onto a chromosome 2, may explain the finding of a der(2)(2pter->2q37::12q24->12q14:) with two FISH fusion signals on it.

Paracentric inversions inv(12)(q14q24) affecting the *HMGA2* gene have been reported in chondroid hamartomas, endometrial polyps, and lipomas (34-39). Fusion of *HMGA2* with aldehyde dehydrogenase 2 family member gene (*ALDH2*) was also reported, in a uterine leiomyoma, as the result of a cryptic inv(12)(q14q24) (34).

Alternatively, more complex chromosomal aberrations involving double breaks upstream and in intron 3 or 4 of *HMGA2* together with breaks in the 5'-end region of *NCOR2* would generate an *HMGA2-NCOR2* fusion gene at 12q24. There is no cytogenetic evidence at hand, however, pointing to the actual existence of these potential cytogenetic ways of obtaining *HMGA2* rearrangements in connective tissue tumors.

This notwithstanding, many chromosomal rearrangements, such as balanced and unbalanced translocations, inversions, insertions, and deletions involving band 12q14 and targeting the *HMGA2* gene have repeatedly been reported in lipomas and other benign neoplasms of connective tissues (40). In most cases, *HMGA2* fuses out-of-frame with the 3'-end partner gene or with intergenic sequences (32, 34, 36, 41-53). In these fusions, the part of the *HMGA2* gene coding for the AT-hook domains, *i.e.*, exons 1 to 3, is separated from the 3'-untranslated region which regulates *HMGA2* transcription, resulting in expression and translation of a tumorigenic, truncated form of *HMGA2* (54-60). Thus, the addition of ectopic fusion sequences does not seem to have any significant impact compared with the tumorigenic properties of truncated *HMGA2* (61).

In some cases, the chromosomal rearrangements result in an *HMGA2* fusion with in-frame transcripts coding for chimeric *HMGA2* proteins. The chromosomal translocation t(3;12)(q28;q14) repeatedly found in lipomas (especially) but also chondroid hamartomas and chondromas, fuses in-frame *HMGA2* with a gene whose official full name is LIM domain-containing preferred translocation partner in lipoma (*LPP*) (47, 62-68). The resulting chimera codes for an *HMGA2-LPP* protein containing the AT-hook domains of *HMGA2* and the LIM domains of the *LPP* protein (47, 62-70).

Fusion of *HMGA2* with epidermal growth factor receptor gene (*EGFR*) from 7p11 gives rise to a fusion gene which encodes a chimeric *HMGA2-EGFR* protein; this was reported in a single case of glioblastoma (71). An in-frame fusion transcript of *HMGA2* with Yes1-associated transcriptional regulator gene (*YAP1*) from 11q22 was reported in an aggressive angiomyxoma (72).

Each of the above-mentioned partners is involved in different cell functions and all have been implicated in tumor development. *LPP* belongs to the zyxin family of LIM domain proteins, has focal adhesion capacity, is a transcription activator, interacts with various proteins through its numerous protein-protein interactions domains, and is known to play a role in many biological and cellular processes (69, 73-75). In a secondary acute myeloid leukemia with a t(3;11)(q28;q23) chromosomal translocation, *LPP* fused to lysine methyltransferase 2A (*KMT2A*, formerly *MLL*) generating a *KMT2A-LPP* fusion gene which codes for a chimeric protein containing the AT hook of *KMT2A* and the LIM domains of *LPP* (76). *LPP* was found to be involved in tumor cell migration, invasion, and metastasis (75). *EGFR* is a transmembrane glycoprotein, a member of the protein kinase superfamily, and a receptor for members of the EGF family (77). Mutation and amplification/overexpression of *EGFR* and its protein have been reported in lung cancer and brain tumors (77). *YAP1* is a transcriptional co-activator which affects the Hippo signaling pathway (78-80). Mutations, amplifications, and fusion genes of *YAP1* have been reported in various types of cancer (78-80).

Table IV. *Continued*

Case	Grep search term	Sequences
	CCTGCTCAGCAGCAACAA	<p>CAGCAGCAACAACAGCAGCAGCAGCGGCCAAGAGGCAGACCTAGGAAATGGCCACAA CAAGTTGTTTCAGAAGAAGCCTGCTCAGCAGCAGCAACAACAGCAGGCCACAACAAGT TGTTTCAGAAGAAGCCTGCTCAGCAGCAGCAACAACAGCAGCAGCAGCAGCAGCAGCA GCAGCATAGGAAATGGCCACAACAAGTTGTTTCAGAAGAAGCCTGCTCAGCAGCAGC AACAACAGCAGCAGCAGCAGCAGCAG</p> <p>AAAACGGCCAAGAGGCAGACCTAGGAAATGGCCACAACAAGTTGTTTCAGAAGAA GCCTGCTCAGCAGCAACAACAGAAAACGGCCAAGAGGCAGACCTAGGAAATGG CCACAACAAGTTGTTTCAGAAGAAGCCTGCTCAGCAGCAACAACAACAAGTTGTT CAGAAGAAGCCTGCTCAGCAGCAACAACAGCAGCAGCAGCAGCAGCAGCAGCAG CAGCAGCAGCAGCCAATGGCCACAACAAGTTGTTTCAGAAGAAGCCTGCTCAGCAG CAACAACAGCAGCAGCAGCAGCAGCAGCAGCAGCAACGGCCAAGAGGCAGACCTA GGAAATGGCCACAACAAGTTGTTTCAGAAGAAGCCTGCTCAGCAGCAACAACAGCAG AGAAAAACGGCCAAGAGGCAGACCTAGGAAATGGCCACAACAAGTTGTTTCAGA AGAAGCCTGCTCAGCAGCAACAAGGCAGACCTAGGAAATGGCCACAACAAGTT GTTTCAGAAGAAGCCTGCTCAGCAGCAACAACAGCAGCAGCAGCAGCAGCAGAAGAAG CCTGCTCAGCAGCAACAACAGCAGCAGCAGCAGCAGCAGCAGCAGCAGCAGCAGCA GCCCATGCCCCCACAACAAGTTGTTTCAGAAGAAGCCTGCTCAGCAGCAACAACAG CAGCAGCAGCAGCAGCAGCAGCAGCAGCAGCGAAGAAGCCTGCTCAGCAGCAACAA CAGCAGCAGCAGCAGCAGCAGCAGCAGCAGCAGCAGCAGCAGCAGCAGCAGCAGCAGC CATGCCCCGACAGCGCCAAGAGGCAGACCTAGGAAATGGCCACAACAAGTTGTTTCAGA AGAAGCCTGCTCAGCAGCAACAACAGCAGCAGGGAAATGGCCACAACAAGTTGTTCA GAAGAAGCCTGCTCAGCAGCAACAACAGCAGCAGCAGCAGCAGCAGCAGCAGCAGCAGC CCTAGGAAATGGCCACAACAAGTTGTTTCAGAAGAAGCCTGCTCAGCAGCAACAACAGC AGCAGCAGCAGCGTTGTTTCAGAAGAAGCCTGCTCAGCAGCAACAACAGCAGCAGCAGC AGCAGCAGCAGCAGCAGCAGCAGCAGCCATAGGAAATGGCCACAACAACAAGTTGTTTCAG AAGAAGCCTGCTCAGCAGCAACAACAGCAGCAGCAGCAGCAGCAGCAGCAGCAGCAGCAG</p>

Tumorigenic properties were found for the HMGA2–LPP and HMGA2–EGFR fusion proteins, whereas functional studies have not been performed to test for effects of the HMGA2–YAP1 chimera (54, 70-72). HMGA2–LPP transforms 3T3 mouse embryonic fibroblasts (54). HMGA2–LPP was also found to act as a transcription activator stimulated by co-expression of HMGA2 (70). Furthermore, it was shown that through the AT-hook DNA-binding domains of HMGA2, HMGA2–LPP transactivates the promoter of collagen type XI alpha 2 chain (*COL11A2*) gene and, consequently, promotes chondrogenesis (81).

The HMGA2–EGFR chimeric protein, which contains the AT-hook domains of HMGA2 and transmembrane and kinase domains of EGFR, showed transforming potential, significantly enhancing colony formation in soft agar (71). Implantation of cells expressing HMGA2–EGFR into mice resulted in accelerated tumor growth (71).

The *HMGA2-NCOR2* chimeric gene we describe here is the fourth fusion coding for a chimeric protein. Based on the *HMGA2* reference sequences NM_003483.4/NP_003474.1 and the *NCOR2* reference sequences NM_006312.6/NP_006303.4, the *HMGA2-NCOR2* fusion transcripts would code for chimeric proteins composed of the first 83 amino acid residues of HMGA2 (or the first 93 amino acids encoded by the

HMGA2 exon 4-*NCOR2* exon 16 fusion) and the last 2021 amino acids of NCOR2 protein (amino acids 494-2514 in NP_006303.4). The chimeric HMGA2–NCOR2 protein thus contains the three regions of HMGA2 (AT-hooks) which bind to the minor groove of adenine-thymine (AT)-rich DNA: AT-hook 1 between amino acid residues 24-34, AT-hook 2 between amino acid residues 44-54, and AT-hook 3 between amino acid residues 71-82 (82-84). It would also contain all functional and interaction domains of NCOR2 except the first *N*-terminal repressor domain (RD1) and the deacetylase activation domain (absence of NCOR2 amino acid residues 1-493). Thus, it contains the histone interaction domain, the RD2 and RD3 repressor domains, the two nuclear receptor interaction domains, and RID1 and RID2 (85-87).

While we were working on the present project, a publication appeared reporting the finding of an *HMGA2-NCOR2* fusion gene in six giant cell-rich soft tissue tumors which expressed low- to high-molecular-weight keratins (the tumor cells stained positively with the immunohistochemical marker cytokeratin AE1/AE3, which is a mixture of two different clones of monoclonal antibodies to cytokeratin AE1 and AE3) (88). In four of the tumors, exon 3 of *HMGA2* fused to exon 16 of *NCOR2*, *i.e.*, the fusion transcript was identical to that found by us in case 1. In the other two

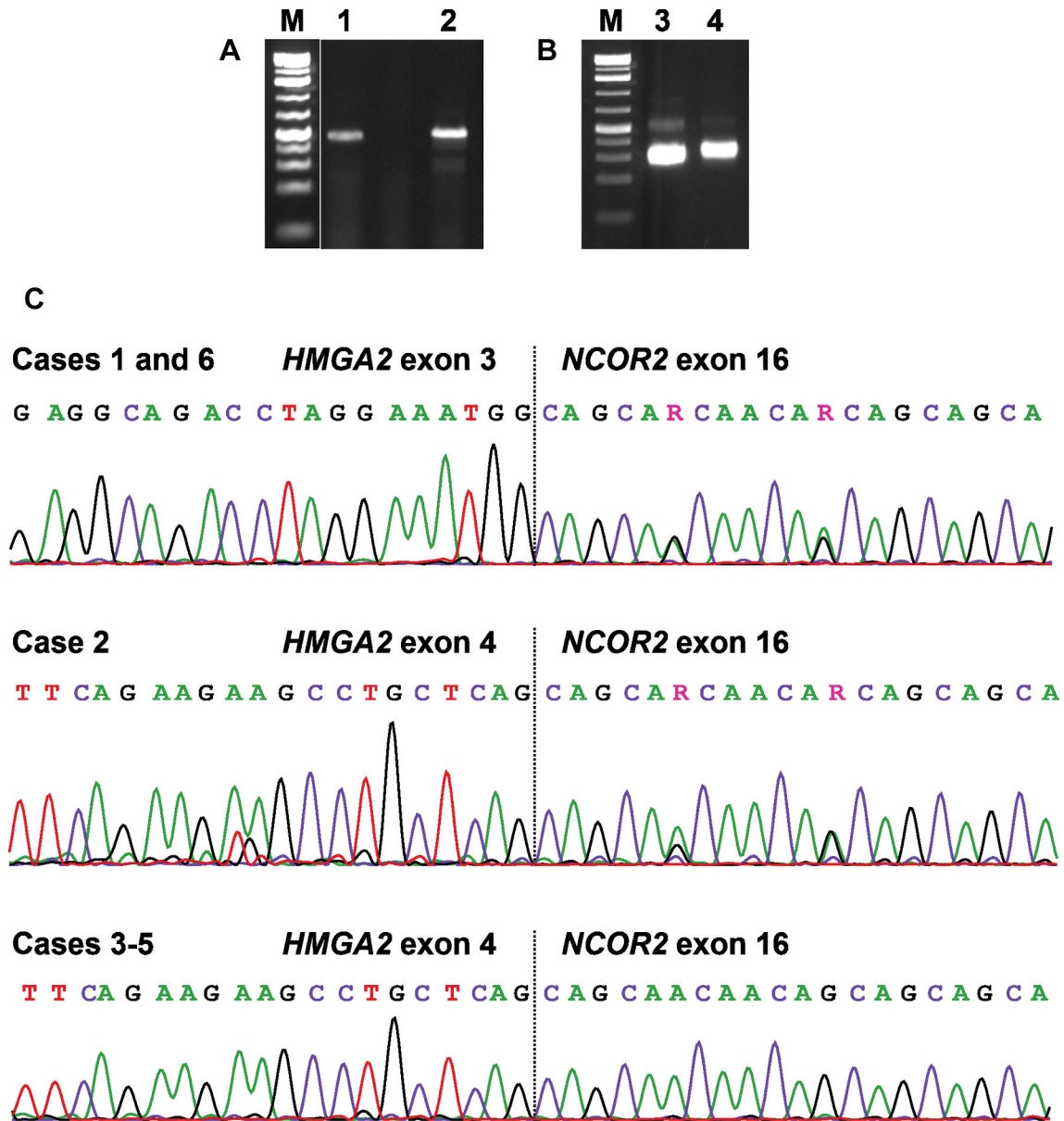


Figure 4. Reverse transcription polymerase chain reaction (PCR) and Sanger sequencing of the osteoclastic giant cell-rich tumors of bone. A: Gel electrophoresis showing amplified high-mobility group AT-hook 2 and nuclear receptor co-repressor 2 fusion (*HMGA2-NCOR2*) cDNA fragments using the outer primer combination *HMGA2-846F1/NCOR2-2127R1* for cases 1 (lane 1) and 2 (lane 2). B: Gel electrophoresis showing amplified *HMGA2-NCOR2* cDNA fragments with nested PCR using the inner primer combination *HMGA2-925F1/NCOR2-2076R1* for cases 1 (lane 3) and 2 (lane 4). M: GeneRuler 1 kb Plus DNA ladder (ThermoFisher Scientific). C: Partial sequence chromatograms of cDNA amplified fragments from cases 1 and 6, case 2, and cases 3-5 showing the junction between *HMGA2* and *NCOR2*. In cases 1 and 6, exon 3 of *HMGA2* was fused to exon 16 of *NCOR2*. In cases 2 to 5, exon 4 of *HMGA2* was fused to exon 16 of *NCOR2*. In cases 1, 2, and 6, there was an in-frame insertion/deletion of a CAG triplet in exon 16 of *NCOR2* at the junction of the fusion transcripts. For this reason, the *NCOR2* sequence at the junction is CAGCARCAACARCAGCAGCA. The letter R in exon 16 of *NCOR2* indicates nucleotide G or A.

tumors, exon 3 of *HMGA2* fused in-frame to exon 20 of *NCOR2* (88). Thus, both studies, the present and that published by Agaimy and coworkers (88), showed *HMGA2-NCOR2* fusion genes coding for similar chimeric proteins

and that a group of giant cell-rich tumors of bone or soft tissue are characterized by the *HMGA2-NCOR2* fusion gene. Our study, furthermore, presents the first cytogenetic evidence, also obtained by FISH analyses, of this fusion.

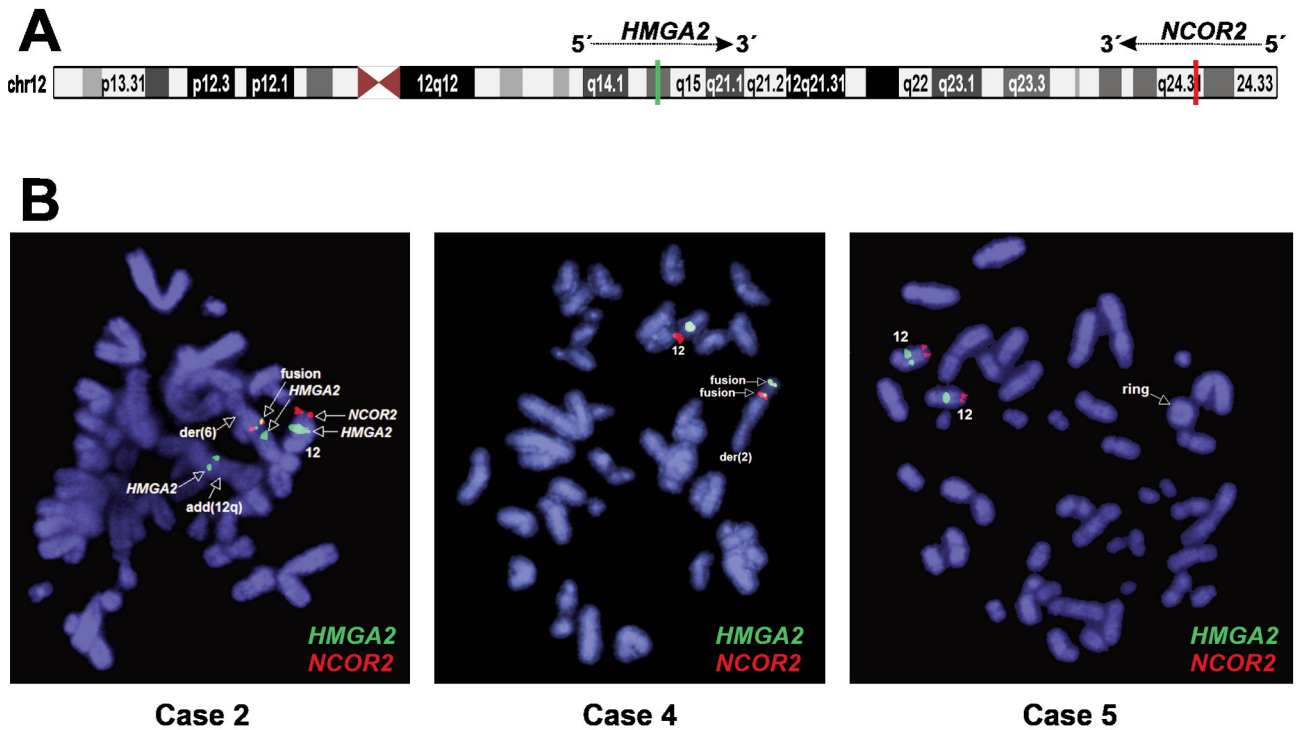


Figure 5. Fluorescence in situ hybridization (FISH) analysis of osteoclastic giant cell-rich tumors of bone using double-fusion FISH probes. A: The position and the orientation of transcription (5'→3') of the high-mobility group AT-hook 2 (*HMGA2*; green label) and nuclear receptor co-repressor 2 (*NCOR2*; red label) genes are shown on the ideogram of chromosome 12. B: FISH results on metaphase spreads from cases 2, 4, and 5. The probes for *HMGA2* were labelled with fluorescein-12-dCTP to obtain green signals. The probes for *NCOR2* were labelled with Texas Red-5-dCTP to obtain a red signal. Case 2: A yellow signal for *HMGA2–NCOR2* fusion together with a green signal for *HMGA2* were detected on the der(6)(6pter→6q21::12q13→12q?::12q24→12q14:). Green signals for *HMGA2* were found on chromosomes 12 and add(12)(q13). A red signal for *NCOR2* was found on chromosome 12. Case 4: Two fusion signals were found on der(2)(2pter→2q37::12q24→12q14:) together with a green signal for *HMGA2* and a red signal for *NCOR2* on chromosome 12. Case 5: A metaphase spread with ring chromosome showing green (*HMGA2*) and red (*NCOR2*) signals on the two chromosomes 12 indicating that the *HMGA2–NCOR2* fusion must have been formed in another, undetected cytogenetic clone.

An in-frame *HMGA2–NCOR2* fusion transcript was also reported in a tenosynovial giant-cell tumor without any information on the fusion junction (89). However, the data indicate that the *HMGA2–NCOR2* pathogenetic pathway might also be found in other types of neoplasia.

The tumors with *HMGA2–NCOR2* of the present study belonged to the group of osteoclastic giant cell-rich tumors; they were initially diagnosed as giant cell tumors of bone negative for H3.3 G35W (1, 2) and difficult to distinguish from non-ossifying fibromas. We believe that the *HMGA2–NCOR2* fusion transcript can be used as a differential diagnostic marker useful in subdividing various osteoclastic giant cell-rich tumors.

Conflicts of Interest

The Authors declare that they have no potential conflicts of interest in regard to this study.

Authors' Contributions

IP designed and supervised the research, performed molecular genetic experiments and bioinformatics analysis, and wrote the article. LG performed cytogenetic analysis. KA performed cytogenetic analysis, molecular genetic experiments, and evaluated the data. ML-I performed pathological examination. IL performed pathological examination. SH evaluated the cytogenetic data and assisted in writing the article. All authors read and approved of the final article.

Acknowledgements

This work was supported by grants from Radiumhospitalets Legater.

References

- 1 WHO Classification of Tumours Editorial Board: WHO classification of Tumours of Soft Tissue and Bone. Fifth Edition. Lyon, France, International Agency for Research on Cancer, 2020.

- 2 Choi JH and Ro JY: The 2020 WHO classification of tumors of bone: an updated review. *Adv Anat Pathol* 28(3): 119-138, 2021. PMID: 33480599. DOI: 10.1097/PAP.0000000000000293
- 3 Oliveira AM, Hsi BL, Weremowicz S, Rosenberg AE, Dal Cin P, Joseph N, Bridge JA, Perez-Atayde AR and Fletcher JA: *USP6* (*Tre2*) fusion oncogenes in aneurysmal bone cyst. *Cancer Res* 64(6): 1920-1923, 2004. PMID: 15026324. DOI: 10.1158/0008-5472.can-03-2827
- 4 Oliveira AM, Perez-Atayde AR, Inwards CY, Medeiros F, Derr V, Hsi BL, Gebhardt MC, Rosenberg AE and Fletcher JA: *USP6* and *CDH11* oncogenes identify the neoplastic cell in primary aneurysmal bone cysts and are absent in so-called secondary aneurysmal bone cysts. *Am J Pathol* 165(5): 1773-1780, 2004. PMID: 15509545. DOI: 10.1016/S0002-9440(10)63432-3
- 5 Oliveira AM, Perez-Atayde AR, Dal Cin P, Gebhardt MC, Chen CJ, Neff JR, Demetri GD, Rosenberg AE, Bridge JA and Fletcher JA: Aneurysmal bone cyst variant translocations upregulate *USP6* transcription by promoter swapping with the *ZNF9*, *COL1A1*, *TRAP150*, and *OMD* genes. *Oncogene* 24(21): 3419-3426, 2005. PMID: 15735689. DOI: 10.1038/sj.onc.1208506
- 6 Šekoranja D, Boštančić E, Salapura V, Mavčič B and Pižem J: Primary aneurysmal bone cyst with a novel *SPARC-USP6* translocation identified by next-generation sequencing. *Cancer Genet* 228-229: 12-16, 2018. PMID: 30553465. DOI: 10.1016/j.cancergen.2018.07.001
- 7 Panagopoulos I, Gorunova L, Andersen K, Lobmaier I, Lund-Iversen M, Micci F and Heim S: Fusion of the lumican (*LUM*) gene with the ubiquitin specific peptidase 6 (*USP6*) gene in an aneurysmal bone cyst carrying a t(12;17)(q21;p13) chromosome translocation. *Cancer Genomics Proteomics* 17(5): 555-561, 2020. PMID: 32859633. DOI: 10.21873/cgp.20211
- 8 Šekoranja D, Zupan A, Mavčič B, Martinčič D, Salapura V, Snož Ž, Limpel Novak AK and Pižem J: Novel *ASAPI-USP6*, *FAT1-USP6*, *SARIA-USP6*, and *TNC-USP6* fusions in primary aneurysmal bone cyst. *Genes Chromosomes Cancer* 59(6): 357-365, 2020. PMID: 32011035. DOI: 10.1002/gcc.22836
- 9 Panoutsakopoulos G, Pandis N, Kyriazoglou I, Gustafson P, Mertens F and Mandahl N: Recurrent t(16;17)(q22;p13) in aneurysmal bone cysts. *Genes Chromosomes Cancer* 26(3): 265-266, 1999. PMID: 10502326. DOI: 10.1002/(sici)1098-2264(199911)26:3<265::aid-gcc12>3.0.co;2-#
- 10 Baumhoer D, Kovac M, Sperveslage J, Ameline B, Strobl AC, Krause A, Trautmann M, Wardelmann E, Nathrath M, Höller S, Harges J, Gosheger G, Krieg AH, Vieth V, Tirabosco R, Amary F, Flanagan AM and Hartmann W: Activating mutations in the MAP-kinase pathway define non-ossifying fibroma of bone. *J Pathol* 248(1): 116-122, 2019. PMID: 30549028. DOI: 10.1002/path.5216
- 11 Bovée JV and Hogendoorn PC: Non-ossifying fibroma: A RAS-MAPK driven benign bone neoplasm. *J Pathol* 248(2): 127-130, 2019. PMID: 30809793. DOI: 10.1002/path.5259
- 12 Behjati S, Tarpey PS, Presneau N, Scheipl S, Pillay N, Van Loo P, Wedge DC, Cooke SL, Gundem G, Davies H, Nik-Zainal S, Martin S, McLaren S, Goodie V, Robinson B, Butler A, Teague JW, Halai D, Khatri B, Myklebost O, Baumhoer D, Jundt G, Hamoudi R, Tirabosco R, Amary MF, Futreal PA, Stratton MR, Campbell PJ and Flanagan AM: Distinct *H3F3A* and *H3F3B* driver mutations define chondroblastoma and giant cell tumor of bone. *Nat Genet* 45(12): 1479-1482, 2013. PMID: 24162739. DOI: 10.1038/ng.2814
- 13 Cleven AH, Höcker S, Briaire-de Bruijn I, Szuhai K, Cleton-Jansen AM and Bovée JV: Mutation analysis of *H3F3A* and *H3F3B* as a diagnostic tool for giant cell tumor of bone and chondroblastoma. *Am J Surg Pathol* 39(11): 1576-1583, 2015. PMID: 26457357. DOI: 10.1097/PAS.0000000000000512
- 14 Presneau N, Baumhoer D, Behjati S, Pillay N, Tarpey P, Campbell PJ, Jundt G, Hamoudi R, Wedge DC, Loo PV, Hassan AB, Khatri B, Ye H, Tirabosco R, Amary MF and Flanagan AM: Diagnostic value of *H3F3A* mutations in giant cell tumour of bone compared to osteoclast-rich mimics. *J Pathol Clin Res* 1(2): 113-123, 2015. PMID: 27499898. DOI: 10.1002/cjp.2.13
- 15 Kervarrec T, Collin C, Larousserie F, Bouvier C, Aubert S, Gomez-Brouchet A, Marie B, Miquelstarena-Standley E, Le Nail LR, Avril P, Christophe Pagès J and de Pinieux G: *H3F3* mutation status of giant cell tumors of the bone, chondroblastomas and their mimics: a combined high resolution melting and pyrosequencing approach. *Mod Pathol* 30(3): 393-406, 2017. PMID: 28059095. DOI: 10.1038/modpathol.2016.212
- 16 Ogura K, Hosoda F, Nakamura H, Hama N, Totoki Y, Yoshida A, Ohashi S, Rokutan H, Takai E, Yachida S, Kawai A, Tanaka S and Shibata T: Highly recurrent *H3F3A* mutations with additional epigenetic regulator alterations in giant cell tumor of bone. *Genes Chromosomes Cancer* 56(10): 711-718, 2017. PMID: 28545165. DOI: 10.1002/gcc.22469
- 17 Righi A, Mancini I, Gambarotti M, Picci P, Gamberi G, Marraccini C, Dei Tos AP, Simi L, Pinzani P and Franchi A: Histone 3.3 mutations in giant cell tumor and giant cell-rich sarcomas of bone. *Hum Pathol* 68: 128-135, 2017. PMID: 28899740. DOI: 10.1016/j.humpath.2017.08.033
- 18 Gamberi G, Morandi L, Benini S, Resca A, Cocchi S, Magagnoli G, Donati DM, Righi A and Gambarotti M: Detection of *H3F3A* p.G35W and p.G35R in giant cell tumor of bone by Allele Specific Locked Nucleic Acid quantitative PCR (ASLNAqPCR). *Pathol Res Pract* 214(1): 89-94, 2018. PMID: 29254795. DOI: 10.1016/j.prp.2017.10.023
- 19 Leske H, Rushing E, Budka H, Niehusmann P, Pahnke J and Panagopoulos I: K27/G34 versus K28/G35 in histone H3-mutant gliomas: A note of caution. *Acta Neuropathol* 136(1): 175-176, 2018. PMID: 29766298. DOI: 10.1007/s00401-018-1867-2
- 20 Leske H, Dalgleish R, Lazar AJ, Reifemberger G and Cree IA: A common classification framework for histone sequence alterations in tumours: an expert consensus proposal. *J Pathol* 254(2): 109-120, 2021. PMID: 33779999. DOI: 10.1002/path.5666
- 21 Panagopoulos I, Gorunova L, Lund-Iversen M, Andersen K, Andersen HK, Lobmaier I, Bjerkehagen B and Heim S: Cytogenetics of spindle cell/pleomorphic lipomas: Karyotyping and FISH analysis of 31 tumors. *Cancer Genomics Proteomics* 15(3): 193-200, 2018. PMID: 29695401. DOI: 10.21873/cgp.20077
- 22 Mandahl N: Methods in solid tumour cytogenetics. In: *Human Cytogenetics: Malignancy and Acquired Abnormalities*. Rooney DE (ed.). New York, Oxford University Press, pp. 165-203, 2001.
- 23 McGowan-Jordan J, Simons A and Schmid M: ISCN 2016: An International System for Human Cytogenomic Nomenclature. Basel, Karger, pp. 140, 2016.
- 24 Kangaspeska S, Hultsch S, Edgren H, Nicorici D, Murumägi A and Kallioniemi O: Reanalysis of RNA-sequencing data reveals several additional fusion genes with multiple isoforms. *PLoS One* 7(10): e48745, 2012. PMID: 23119097. DOI: 10.1371/journal.pone.0048745

- 25 Nicorici D, Satalan M, Edgren H, Kangaspeska S, Murumagi A, Kallioniemi O, Virtanen S and Kilkku O: FusionCatcher - a tool for finding somatic fusion genes in paired-end RNA-sequencing data. *bioRxiv*, 2014. DOI: 10.1101/011650
- 26 Panagopoulos I, Torkildsen S, Gorunova L, Tierens A, Tjønnfjord GE and Heim S: Comparison between karyotyping-FISH-reverse transcription PCR and RNA-sequencing-fusion gene identification programs in the detection of *KAT6A-CREBBP* in acute myeloid leukemia. *PLoS One* 9(5): e96570, 2014. PMID: 24798186. DOI: 10.1371/journal.pone.0096570
- 27 Panagopoulos I, Gorunova L, Bjerkehagen B and Heim S: The “grep” command but not FusionMap, FusionFinder or ChimeraScan captures the *CIC-DUX4* fusion gene from whole transcriptome sequencing data on a small round cell tumor with t(4;19)(q35;q13). *PLoS One* 9(6): e99439, 2014. PMID: 24950227. DOI: 10.1371/journal.pone.0099439
- 28 Panagopoulos I, Gorunova L, Bjerkehagen B and Heim S: Novel *KAT6B-KANSL1* fusion gene identified by RNA sequencing in retroperitoneal leiomyoma with t(10;17)(q22;q21). *PLoS One* 10(1): e0117010, 2015. PMID: 25621995. DOI: 10.1371/journal.pone.0117010
- 29 Panagopoulos I, Gorunova L, Lund-Iversen M, Bassarova A and Heim S: Fusion of the genes *PHF1* and *TFE3* in malignant chondroid syringoma. *Cancer Genomics Proteomics* 16(5): 345-351, 2019. PMID: 31467228. DOI: 10.21873/cgp.20139
- 30 Panagopoulos I, Gorunova L, Andersen K, Lund-Iversen M, Lobmaier I, Micci F and Heim S: *NDRG1-PLAG1* and *TRPS1-PLAG1* fusion genes in chondroid syringoma. *Cancer Genomics Proteomics* 17(3): 237-248, 2020. PMID: 32345665. DOI: 10.21873/cgp.20184
- 31 Altschul SF, Gish W, Miller W, Myers EW and Lipman DJ: Basic local alignment search tool. *J Mol Biol* 215(3): 403-410, 1990. PMID: 2231712. DOI: 10.1016/S0022-2836(05)80360-2
- 32 Panagopoulos I, Bjerkehagen B, Gorunova L, Taksdal I and Heim S: Rearrangement of chromosome bands 12q14~15 causing *HMGA2-SOX5* gene fusion and *HMGA2* expression in extraskeletal osteochondroma. *Oncol Rep* 34(2): 577-584, 2015. PMID: 26043835. DOI: 10.3892/or.2015.4035
- 33 Pandis N, Bardi G, Sfikas K, Panayotopoulos N, Tserkezoglou A and Fotiou S: Complex chromosome rearrangements involving 12q14 in two uterine leiomyomas. *Cancer Genet Cytogenet* 49(1): 51-56, 1990. PMID: 2397473. DOI: 10.1016/0165-4608(90)90163-5
- 34 Kazmierczak B, Hennig Y, Wanschura S, Rogalla P, Bartnitzke S, Van de Ven W and Bullerdiek J: Description of a novel fusion transcript between *HMGI-C*, a gene encoding for a member of the high mobility group proteins, and the mitochondrial aldehyde dehydrogenase gene. *Cancer Res* 55(24): 6038-6039, 1995. PMID: 8521389.
- 35 Wanschura S, Dal Cin P, Kazmierczak B, Bartnitzke S, Van den Berghe H and Bullerdiek J: Hidden paracentric inversions of chromosome arm 12q affecting the *HMGIC* gene. *Genes Chromosomes Cancer* 18(4): 322-323, 1997. PMID: 9087575.
- 36 Kazmierczak B, Dal Cin P, Wanschura S, Bartnitzke S, Van den Berghe H and Bullerdiek J: Cloning and molecular characterization of part of a new gene fused to *HMGIC* in mesenchymal tumors. *Am J Pathol* 152(2): 431-435, 1998. PMID: 9466569.
- 37 Kazmierczak B, Meyer-Bolte K, Tran KH, Wöckel W, Breightman I, Rosigkeit J, Bartnitzke S and Bullerdiek J: A high frequency of tumors with rearrangements of genes of the *HMGI(Y)* family in a series of 191 pulmonary chondroid hamartomas. *Genes Chromosomes Cancer* 26(2): 125-133, 1999. PMID: 10469450.
- 38 Weremowicz S and Morton CC: Is *HMGIC* rearranged due to cryptic paracentric inversion of 12q in karyotypically normal uterine leiomyomas? *Genes Chromosomes Cancer* 24(2): 172-173, 1999. PMID: 9885987. DOI: 10.1002/(sici)1098-2264(199902)24:2<172::aid-gcc13>3.0.co;2-z
- 39 Bartuma H, Panagopoulos I, Collin A, Trombetta D, Domanski HA, Mandahl N and Mertens F: Expression levels of *HMGA2* in adipocytic tumors correlate with morphologic and cytogenetic subgroups. *Mol Cancer* 8: 36, 2009. PMID: 19508721. DOI: 10.1186/1476-4598-8-36
- 40 Unachukwu U, Chada K and D’Armiento J: High mobility group AT-Hook 2 (*HMGA2*) oncogenicity in mesenchymal and epithelial neoplasia. *Int J Mol Sci* 21(9): 3151, 2020. PMID: 32365712. DOI: 10.3390/ijms21093151
- 41 Geurts JM, Schoenmakers EF, Røijer E, Aström AK, Stenman G and van de Ven WJ: Identification of *NFIB* as recurrent translocation partner gene of *HMGIC* in pleomorphic adenomas. *Oncogene* 16(7): 865-872, 1998. PMID: 9484777. DOI: 10.1038/sj.onc.1201609
- 42 Mine N, Kurose K, Konishi H, Araki T, Nagai H and Emi M: Fusion of a sequence from *HEI10* (14q11) to the *HMGIC* gene at 12q15 in a uterine leiomyoma. *Jpn J Cancer Res* 92(2): 135-139, 2001. PMID: 11223542. DOI: 10.1111/j.1349-7006.2001.tb01075.x
- 43 Broberg K, Zhang M, Strömbeck B, Isaksson M, Nilsson M, Mertens F, Mandahl N and Panagopoulos I: Fusion of *RDC1* with *HMGA2* in lipomas as the result of chromosome aberrations involving 2q35-37 and 12q13-15. *Int J Oncol* 21(2): 321-326, 2002. PMID: 12118328.
- 44 Nilsson M, Panagopoulos I, Mertens F and Mandahl N: Fusion of the *HMGA2* and *NFIB* genes in lipoma. *Virchows Arch* 447(5): 855-858, 2005. PMID: 16133369. DOI: 10.1007/s00428-005-0037-9
- 45 Odero MD, Grand FH, Iqbal S, Ross F, Roman JP, Vizmanos JL, Andrieux J, Laï JL, Calasanz MJ and Cross NC: Disruption and aberrant expression of *HMGA2* as a consequence of diverse chromosomal translocations in myeloid malignancies. *Leukemia* 19(2): 245-252, 2005. PMID: 15618963. DOI: 10.1038/sj.leu.2403605
- 46 Nilsson M, Mertens F, Höglund M, Mandahl N and Panagopoulos I: Truncation and fusion of *HMGA2* in lipomas with rearrangements of 5q32—>q33 and 12q14—>q15. *Cytogenet Genome Res* 112(1-2): 60-66, 2006. PMID: 16276091. DOI: 10.1159/000087514
- 47 Hatano H, Morita T, Ogose A, Hotta T, Kobayashi H, Segawa H, Uchiyama T, Takenouchi T and Sato T: Clinicopathological features of lipomas with gene fusions involving *HMGA2*. *Anticancer Res* 28(1B): 535-538, 2008. PMID: 18383898.
- 48 Velagaleti GV, Tonk VS, Hakim NM, Wang X, Zhang H, Erickson-Johnson MR, Medeiros F and Oliveira AM: Fusion of *HMGA2* to *COG5* in uterine leiomyoma. *Cancer Genet Cytogenet* 202(1): 11-16, 2010. PMID: 20804914. DOI: 10.1016/j.cancergencyto.2010.06.002
- 49 Martin SE, Sausen M, Joseph A, Kingham BF and Martin ES: Identification of a *HMGA2-EFCAB6* gene rearrangement following next-generation sequencing in a patient with a t(12;22)(q14.3;q13.2) and JAK2V617F-positive myeloproliferative neoplasm. *Cancer*

- Genet 205(6): 295-303, 2012. PMID: 22749035. DOI: 10.1016/j.cancergen.2012.03.006
- 50 Bianchini L, Birtwisle L, Saáda E, Bazin A, Long E, Roussel JF, Michiels JF, Forest F, Dani C, Myklebost O, Birtwisle-Peyrottes I and Pedetour F: Identification of *PPAP2B* as a novel recurrent translocation partner gene of *HMGA2* in lipomas. Genes Chromosomes Cancer 52(6): 580-590, 2013. PMID: 23508853. DOI: 10.1002/gcc.22055
- 51 Panagopoulos I, Gorunova L, Bjerkehagen B, Lobmaier I and Heim S: The recurrent chromosomal translocation t(12;18)(q14~15;q12~21) causes the fusion gene *HMGA2-SETBP1* and *HMGA2* expression in lipoma and osteochondrolipoma. Int J Oncol 47(3): 884-890, 2015. PMID: 26202160. DOI: 10.3892/ijo.2015.3099
- 52 Agostini A, Gorunova L, Bjerkehagen B, Lobmaier I, Heim S and Panagopoulos I: Molecular characterization of the t(4;12)(q27~28;q14~15) chromosomal rearrangement in lipoma. Oncol Lett 12(3): 1701-1704, 2016. PMID: 27588119. DOI: 10.3892/ol.2016.4834
- 53 Panagopoulos I, Gorunova L, Agostini A, Lobmaier I, Bjerkehagen B and Heim S: Fusion of the *HMGA2* and *C9orf92* genes in myolipoma with t(9;12)(p22;q14). Diagn Pathol 11: 22, 2016. PMID: 26857357. DOI: 10.1186/s13000-016-0472-8
- 54 Fedele M, Berlingieri MT, Scala S, Chiariotti L, Viglietto G, Rippel V, Bullerdiek J, Santoro M and Fusco A: Truncated and chimeric *HMGI-C* genes induce neoplastic transformation of NIH3T3 murine fibroblasts. Oncogene 17(4): 413-418, 1998. PMID: 9696033. DOI: 10.1038/sj.onc.1201952
- 55 Arlotta P, Tai AK, Manfioletti G, Clifford C, Jay G and Ono SJ: Transgenic mice expressing a truncated form of the high mobility group I-C protein develop adiposity and an abnormally high prevalence of lipomas. J Biol Chem 275(19): 14394-14400, 2000. PMID: 10747931. DOI: 10.1074/jbc.m000564200
- 56 Borrmann L, Wilkening S and Bullerdiek J: The expression of *HMGA* genes is regulated by their 3'UTR. Oncogene 20(33): 4537-4541, 2001. PMID: 11494149. DOI: 10.1038/sj.onc.1204577
- 57 Lee YS and Dutta A: The tumor suppressor microRNA let-7 represses the *HMGA2* oncogene. Genes Dev 21(9): 1025-1030, 2007. PMID: 17437991. DOI: 10.1101/gad.1540407
- 58 Mayr C, Hemann MT and Bartel DP: Disrupting the pairing between *let-7* and *Hmga2* enhances oncogenic transformation. Science 315(5818): 1576-1579, 2007. PMID: 17322030. DOI: 10.1126/science.1137999
- 59 Kristjánssdóttir K, Fogarty EA and Grimson A: Systematic analysis of the *Hmga2* 3' UTR identifies many independent regulatory sequences and a novel interaction between distal sites. RNA 21(7): 1346-1360, 2015. PMID: 25999317. DOI: 10.1261/rna.051177.115
- 60 Mas A, Cervelló I, Fernández-Álvarez A, Faus A, Díaz A, Burgués O, Casado M and Simón C: Overexpression of the truncated form of High Mobility Group A proteins (HMGA2) in human myometrial cells induces leiomyoma-like tissue formation. Mol Hum Reprod 21(4): 330-338, 2015. PMID: 25542836. DOI: 10.1093/molehr/gau114
- 61 Zaidi MR, Okada Y and Chada KK: Misexpression of full-length HMGA2 induces benign mesenchymal tumors in mice. Cancer Res 66(15): 7453-7459, 2006. PMID: 16885341. DOI: 10.1158/0008-5472.CAN-06-0931
- 62 Ashar HR, Fejzo MS, Tkachenko A, Zhou X, Fletcher JA, Weremowicz S, Morton CC and Chada K: Disruption of the architectural factor HMGI-C: DNA-binding AT hook motifs fused in lipomas to distinct transcriptional regulatory domains. Cell 82(1): 57-65, 1995. PMID: 7606786. DOI: 10.1016/0092-8674(95)90052-7
- 63 Schoenmakers EF, Wanschura S, Mols R, Bullerdiek J, Van den Berghe H and Van de Ven WJ: Recurrent rearrangements in the high mobility group protein gene, *HMGI-C*, in benign mesenchymal tumours. Nat Genet 10(4): 436-444, 1995. PMID: 7670494. DOI: 10.1038/ng0895-436
- 64 Rogalla P, Lemke I, Kazmierczak B and Bullerdiek J: An identical *HMGIC-LPP* fusion transcript is consistently expressed in pulmonary chondroid hamartomas with t(3;12)(q27-28;q14-15). Genes Chromosomes Cancer 29(4): 363-366, 2000. PMID: 11066083.
- 65 Dahlén A, Mertens F, Rydholm A, Brosjö O, Wejde J, Mandahl N and Panagopoulos I: Fusion, disruption, and expression of *HMGA2* in bone and soft tissue chondromas. Mod Pathol 16(11): 1132-1140, 2003. PMID: 14614053. DOI: 10.1097/01.MP.00000092954.42656.94
- 66 Kubo T, Matsui Y, Goto T, Yukata K, Endo K, Sato R, Tsutsui T and Yasui N: MRI characteristics of parosteal lipomas associated with the *HMGA2-LPP* fusion gene. Anticancer Res 26(3B): 2253-2257, 2006. PMID: 16821597.
- 67 Kubo T, Matsui Y, Naka N, Araki N, Goto T, Yukata K, Endo K, Yasui N, Myoui A, Kawabata H, Yoshikawa H and Ueda T: Expression of *HMGA2-LPP* and *LPP-HMGA2* fusion genes in lipoma: identification of a novel type of *LPP-HMGA2* transcript in four cases. Anticancer Res 29(6): 2357-2360, 2009. PMID: 19528502.
- 68 Kubo T, Matsui Y, Naka N, Araki N, Myoui A, Endo K, Yasui N, Ohtani O, Suzuki K, Kimura T, Yoshikawa H and Ueda T: Specificity of fusion genes in adipocytic tumors. Anticancer Res 30(2): 661-664, 2010. PMID: 20332486.
- 69 Petit MM, Mols R, Schoenmakers EF, Mandahl N and Van de Ven WJ: *LPP*, the preferred fusion partner gene of *HMGIC* in lipomas, is a novel member of the LIM protein gene family. Genomics 36(1): 118-129, 1996. PMID: 8812423. DOI: 10.1006/geno.1996.0432
- 70 Crombez KR, Vanoirbeek EM, Van de Ven WJ and Petit MM: Transactivation functions of the tumor-specific HMGA2/LPP fusion protein are augmented by wild-type HMGA2. Mol Cancer Res 3(2): 63-70, 2005. PMID: 15755872. DOI: 10.1158/1541-7786.MCR-04-0181
- 71 Komuro A, Raja E, Iwata C, Soda M, Isogaya K, Yuki K, Ino Y, Morikawa M, Todo T, Aburatani H, Suzuki H, Ranjit M, Natsume A, Mukasa A, Saito N, Okada H, Mano H, Miyazono K and Koinuma D: Identification of a novel fusion gene *HMGA2-EGFR* in glioblastoma. Int J Cancer 142(8): 1627-1639, 2018. PMID: 29193056. DOI: 10.1002/ijc.31179
- 72 Lee MY, da Silva B, Ramirez DC and Maki RG: Novel *HMGA2-YAPI* fusion gene in aggressive angiomyxoma. BMJ Case Rep 12(5): e227475, 2019. PMID: 31142482. DOI: 10.1136/bcr-2018-227475
- 73 Zheng Q and Zhao Y: The diverse biofunctions of LIM domain proteins: determined by subcellular localization and protein-protein interaction. Biol Cell 99(9): 489-502, 2007. PMID: 17696879. DOI: 10.1042/BC20060126
- 74 Grunewald TG, Pasedag SM and Butt E: Cell adhesion and transcriptional activity - defining the role of the novel protooncogene *LPP*. Transl Oncol 2(3): 107-116, 2009. PMID: 19701494. DOI: 10.1593/tlo.09112

- 75 Ngan E, Kiepas A, Brown CM and Siegel PM: Emerging roles for LPP in metastatic cancer progression. *J Cell Commun Signal* 12(1): 143-156, 2018. PMID: 29027626. DOI: 10.1007/s12079-017-0415-5
- 76 Dahéron L, Veinstein A, Brizard F, Drabkin H, Lacotte L, Guilhot F, Larsen CJ, Brizard A and Roche J: Human *LPP* gene is fused to *MLL* in a secondary acute leukemia with a t(3;11)(q28;q23). *Genes Chromosomes Cancer* 31(4): 382-389, 2001. PMID: 11433529. DOI: 10.1002/gcc.1157
- 77 Uribe ML, Marrocco I and Yarden Y: EGFR in cancer: Signaling mechanisms, drugs, and acquired resistance. *Cancers (Basel)* 13(11): 2748, 2021. PMID: 34206026. DOI: 10.3390/cancers13112748
- 78 Shibata M, Ham K and Hoque MO: A time for YAP1: Tumorigenesis, immunosuppression and targeted therapy. *Int J Cancer* 143(9): 2133-2144, 2018. PMID: 29696628. DOI: 10.1002/ijc.31561
- 79 Thompson BJ: YAP/TAZ: Drivers of tumor growth, metastasis, and resistance to therapy. *Bioessays* 42(5): e1900162, 2020. PMID: 32128850. DOI: 10.1002/bies.201900162
- 80 Szulzewsky F, Holland EC and Vasioukhin V: YAP1 and its fusion proteins in cancer initiation, progression and therapeutic resistance. *Dev Biol* 475: 205-221, 2021. PMID: 33428889. DOI: 10.1016/j.ydbio.2020.12.018
- 81 Kubo T, Matsui Y, Goto T, Yukata K and Yasui N: Overexpression of *HMGA2-LPP* fusion transcripts promotes expression of the alpha 2 type XI collagen gene. *Biochem Biophys Res Commun* 340(2): 476-481, 2006. PMID: 16375854. DOI: 10.1016/j.bbrc.2005.12.042
- 82 Reeves R and Nissen MS: The A.T-DNA-binding domain of mammalian high mobility group I chromosomal proteins. A novel peptide motif for recognizing DNA structure. *J Biol Chem* 265(15): 8573-8582, 1990. PMID: 1692833.
- 83 Cattaruzzi G, Altamura S, Tessari MA, Rustighi A, Giancotti V, Pucillo C and Manfioletti G: The second AT-hook of the architectural transcription factor *HMGA2* is determinant for nuclear localization and function. *Nucleic Acids Res* 35(6): 1751-1760, 2007. PMID: 17324944. DOI: 10.1093/nar/gkl1106
- 84 Krahn N, Meier M, To V, Booy EP, McEleney K, O'Neil JD, McKenna SA, Patel TR and Stetefeld J: Nanoscale assembly of high-mobility group AT-Hook 2 protein with DNA replication fork. *Biophys J* 113(12): 2609-2620, 2017. PMID: 29262356. DOI: 10.1016/j.bpj.2017.10.026
- 85 Watson PJ, Fairall L and Schwabe JW: Nuclear hormone receptor co-repressors: structure and function. *Mol Cell Endocrinol* 348(2): 440-449, 2012. PMID: 21925568. DOI: 10.1016/j.mce.2011.08.033
- 86 Liang N, Jakobsson T, Fan R and Treuter E: The nuclear receptor-co-repressor complex in control of liver metabolism and disease. *Front Endocrinol (Lausanne)* 10: 411, 2019. PMID: 31293521. DOI: 10.3389/fendo.2019.00411
- 87 Kang Z and Fan R: PPAR α and NCOR/SMRT corepressor network in liver metabolic regulation. *FASEB J* 34(7): 8796-8809, 2020. PMID: 32396271. DOI: 10.1096/fj.202000055RR
- 88 Agaimy A, Michal M, Stoehr R, Ferrazzi F, Fabian P, Michal M, Franchi A, Haller F, Folpe AL and Kösemehmetoğlu K: Recurrent novel *HMGA2-NCOR2* fusions characterize a subset of keratin-positive giant cell-rich soft tissue tumors. *Mod Pathol* 34(8): 1507-1520, 2021. PMID: 33742141. DOI: 10.1038/s41379-021-00789-8
- 89 Brahmī M, Alberti L, Tirode F, Karanian M, Eberst L, Pissaloux D, Cassier P and Blay JY: Complete response to CSF1R inhibitor in a translocation variant of teno-synovial giant cell tumor without genomic alteration of the *CSF1* gene. *Ann Oncol* 29(6): 1488-1489, 2018. PMID: 29668829. DOI: 10.1093/annonc/mdy129

Received November 10, 2021

Revised December 9, 2021

Accepted December 10, 2021